



Bose-Einstein condensation of magnons under coherent pumping by lightLiang Li *Department of Physics and Center for Joint Quantum Studies, School of Science, Tianjin University, Tianjin 300350, China*Tianyu Liu **Department of Physics and Center for Joint Quantum Studies, School of Science, Tianjin University, Tianjin 300350, China
and Tianjin Key Laboratory of Low Dimensional Materials Physics and Preparing Technology, Tianjin 300350, China*

(Received 5 March 2024; accepted 9 May 2024; published 31 May 2024)

Coherent pumping of magnons by light in an optomagnonic cavity has been recently reported. Here we propose and model the Bose-Einstein condensation of magnons pumped by a coherent pumping source in an optical cavity composed of a ferromagnetic waveguide. To stabilize the condensation, a large number of $\pm k$ -magnon pairs should be pumped into the cavity. We calculate and analyze the methods of direct pumping and indirect pumping by multiple confined optical modes. The results show that the condensation can be achieved only by the direct pumping with threshold powers less than 1 watt.

DOI: [10.1103/PhysRevB.109.184447](https://doi.org/10.1103/PhysRevB.109.184447)**I. INTRODUCTION**

Bose-Einstein condensation (BEC) [1,2], one of the most extraordinary macroscopic quantum phenomena associated with a large number of bosons in the ground state sharing with the same wave function, has been observed in many systems of bosonic atoms, such as ^4He [3], ^{87}Rb [4], and H [5]. Similar phenomena also occur for bosonic quasiparticles in nonequilibrium state such as photons [6], excitons [7], polaritons [8], and magnons [9]. Among these, magnon BEC (mBEC) in films of yttrium iron garnet (YIG) stands out due to its potential application in quantum information transfer and processing [10] and an optical simulator of gravity for studying gravitational waves and black holes [11,12] at room temperature. Initially, the formation of mBEC is achieved by microwave radiation, which increases the density of magnons to exceed a critical value [9,13,14]. Recently, novel methods of the formation of mBEC were proposed, such as using rapid cooling [15], spin Hall effect [16] and spin current [17]. However, in the aforementioned systems, the detection of the mBEC is performed using Brillouin light scattering (BLS) technique. This raises the question that why not utilize laser to generate mBEC.

In recent years, cavity optomagnonics—a hybrid quantum system combining solid-state magnets with cavity, has been extensively studied for its potential as quantum information platforms [18]. The pioneering study of strong coherent coupling between microwave photons and magnons in YIG by Soykal and Flatté [19] unveiled the field of cavity optomagnonics followed by a series of experimental realizations of strong coherent coupling in optomagnonic cavities [20,21]. The coupling between optical photons and magnons has also been studied in other hybrid systems [22–24]. Šimić *et al.* [24]

theoretically show that the detection of gigahertz magnons in ferro/ferrimagnets with light by inelastic Brillouin light scattering (BLS) can be enhanced in an optical cavity, indicating the excitation of a large number of coherent magnons with high momentum by light. Recently, Zhu *et al.* [25] experimentally enhanced the optomagnetic coupling strength in YIG waveguides by employing two laser beams of different modes through the inverse Faraday effect, leading to the all-optical excitation and detection of coherent magnons. These studies make it possible to excite and detect mBEC by lasers in an optical cavity.

In this paper, we propose an approach to achieving mBEC within an optical cavity hybridized with a YIG waveguide. Based on previous studies [22–24] that apply dual laser beams to generate magnons of single mode via stimulated-Raman-like scattering, we develop two distinct pumping strategies—direct pumping and perpendicular pumping (an indirect pumping)—to excite $\pm k$ -magnon pairs with specific frequencies within a YIG waveguide. The formation of mBEC after pumping relies on the four-magnon interactions. Inspired by previous studies on mBEC formation in infinite ferromagnetic films [26–29], our work delves deeper into understanding the cascade and kinetic instability (KI) processes within an optical cavity environment. We rigorously analyze the conditions and feasibility of mBEC formation, taking into account the optomagnonic interactions that coherently excite magnons within the cavity. Our paper not only advances the theoretical understanding of mBEC but also offers practical pathways for realizing mBEC in optomagnonic systems.

The paper is organized as follows. Section II is devoted to the detailed theoretical model underpinning our approach to generating mBEC within an optical cavity. Firstly, we review the model for generating single-mode magnons in an optical cavity, laying the groundwork for subsequent discussions. Secondly, we elucidate the criteria for establishing stable mBEC, highlighting the necessity of generating magnon pairs

*tianyu_liu@tju.edu.cn

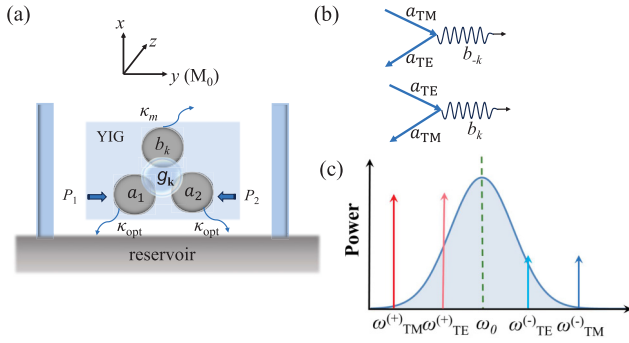


FIG. 1. (a) Schematics of the hybrid system. A static magnetic field is applied along y direction. P_1 and P_2 are two light powers. (b) The Stokes process for $\pm k$ magnon modes. (c) Four laser frequencies relative to ω_0 used in the direct pumping process, where ω_0 is the cavity frequency. $\omega_i^{(\pm)}$ (with $i = \text{TE}, \text{TM}$) refers to the frequency and polarization of the four input lights with “ \pm ” subscript represent the light pair used to pump the $\pm k$ magnon modes.

with $\pm k$ wave vectors. Thirdly, we introduce our method for generating magnon pairs through direct and perpendicular pumping, and provide explicit expressions for the threshold powers required to achieve mBEC formation via the cascade and the KI processes, respectively. In Sec. III we conduct numerical calculations to validate our theoretical framework. Our results demonstrate that the threshold powers of light needed for realizing mBEC in a rectangular ferromagnetic waveguide through coherent pumping are less than 1 watt, thus affirming the feasibility and practicality of our proposed approach. Finally, in Sec. IV, we summarize the key findings and contributions of our paper.

II. MODEL OF MBEC IN CAVITY

A. Pumping magnons by light

In a hybrid system composed of an optical cavity and magnetic YIG waveguide as shown in Fig. 1(a), the gigahertz magnons can be generated through stimulated-Raman-like scattering. By adjusting the frequencies and wave vectors of the incident and the Stokes side-band lights, specific modes of magnons can be obtained, and the number of generated magnons can be controlled by adjusting the input light powers [24].

Here we use the result of Liu *et al.*'s model [23] to deal with the magnon-photon interaction in the hybrid system. The interaction determines the effective field caused by the input light and is of essence in the calculation of threshold powers of light for pumping magnons and forming mBEC in the cavity. The total Hamiltonian can be written in the rotating-wave approximation as

$$H = \hbar\Delta_1 a_1^\dagger a_1 + \hbar\Delta_2 a_2^\dagger a_2 + \sum_k \hbar\omega_k b_k^\dagger b_k + \sum_k \hbar g_k^{(+)} a_1^\dagger a_2^\dagger b_k + \sum_k \hbar g_k^{(-)} a_1^\dagger a_2 b_k^\dagger, \quad (1)$$

where $\Delta_i = \omega_i - \omega_0$ with $i = 1, 2$ denotes the detuning of the input lights frequency from the optical cavity resonance frequency. $g_k^{(\pm)}$ is the photon-magnon coupling strength.

In cavity optomagnonics, a pronounced nonreciprocity and asymmetry exist in the Stokes and the anti-Stokes processes, where $g_k^{(+)}$ is strongly suppressed in the Stokes process while $g_k^{(-)}$ is suppressed in the anti-Stokes process [23,30]. We are interested in generating magnons, and therefore, only $g_k^{(-)}$ is taken into consideration.

According to Šimić *et al.* [24], magnons of frequency ω_k can be generated coherently by applying two laser beams of frequencies ω_1 and ω_2 through stimulated-Raman-like scattering. Although they studied the interactions between magnons in a YIG sphere and laser beams in an optical fiber, their findings are also applicable to our hybridized cavity. We assume $\omega_1 \approx \omega_2 = \omega_{\text{opt}}$ and $P_1 = P_2 = P$, considering the significantly higher frequency of photons compared to magnons. In this case, the coherent magnon number pumped by cavity photons can be expressed as

$$n_k = \frac{P^2}{P_{\text{crit}}^2}, \quad (2)$$

$$P_{\text{crit}} = \frac{\hbar\kappa_m\omega_{\text{opt}}\kappa_{\text{opt}}}{2|g_k|}, \quad (3)$$

where P is the power of input light, κ_m (κ_{opt}) is the magnon (cavity) damping rate, and g_k refers to $g_k^{(-)}$, whose expression has been given in Appendix A as $g_{mm'n}$. In Sec. III, we calculate the maximum coupling strength achievable for $\pm k$ magnon pairs generated by the Stokes process in the optical cavity, where the coupling strength for exciting $+k$ magnons is $g_{+k} = 2\pi \times 27$ Hz and for exciting $-k$ magnons is $g_{-k} = 2\pi \times 12$ Hz. Therefore, the corresponding critical powers required for exciting the two modes are different.

The corresponding classical spin wave amplitude is

$$\tilde{b}_k = \sqrt{n_k} e^{-i\omega_k t}, \quad (4)$$

which will be used later when discussing the threshold power for the formation of mBEC.

B. Stability of mBEC

Since the realization of BEC in alkali metal atoms such as Na [31] and Li [32] at the end of the 20th century, the influence of interactions on cold-atom systems has been a subject of great interest among researchers. Studies [33,34] have shown that the interactions between atoms play a crucial role in the stabilization of BEC. At zero temperature, the BEC of a dilute neutral atom gas can be described by a single wave function $\Phi(\mathbf{r}, t)$, which is a solution to the Gross-Pitaevskii (GP) equation [35,36],

$$i\hbar \frac{\partial}{\partial t} \Phi(\mathbf{r}, t) = \left(-\frac{\hbar^2 \nabla^2}{2m} + V_{\text{ext}}(\mathbf{r}) + g|\Phi(\mathbf{r}, t)|^2 \right) \Phi(\mathbf{r}, t), \quad (5)$$

where m is the atom mass, V_{ext} is the trapped potential, and g is the coupling strength of binary collisions between the atoms. When atom-atom interactions are repulsive ($g > 0$), the system is unconditionally stable; while for attractive interactions ($g < 0$), it will collapse once $|\Phi(\mathbf{r}, t)|^2$ (the atom number) exceeds a certain value.

For quasiparticles like magnons, whose interparticle interactions are much less than their kinetic energy, one can use similar GP equation to study the stability of mBEC. The mass of real atoms in Eq. (5) can be replaced by the effective mass of quasiparticles, and the sign of g can be used to determine the stability of the condensate. For quite a long time, no one is interested in looking for mBEC in ferromagnetic films, since the magnon-magnon interactions dominated by magnetic dipolar interactions are attractive [37], implying that a stable mBEC cannot exist. However, Demokritov *et al.* [9] observed a room-temperature mBEC in a YIG film in 2006, raising a paradox. There was no satisfactory explanation to this contradiction until 2018, when Dzyapko *et al.* [38] provided both theoretical and experimental evidence. The study showed that the mBEC realized in the experiment is a degenerate two-component mBEC, that is the condensation occurs at $\pm k_0$ states simultaneously. The magnons within the same component exhibit a weak attractive interaction, whereas those between different components exhibit a strong repulsive interaction. As a result, the total interaction in the YIG film appears repulsive.

Therefore, to create a stable mBEC in an optical cavity, we have to generate a two-component mBEC, which requires the initial magnons pumped into the system to be $\pm k$ -magnon pairs. We propose two methods to pump magnons with opposite wave vectors. The first one involves applying four laser beams to the cavity to coherently pump two magnons with opposite wave vectors but the same frequency as shown in Fig. 1(c). The second one involves pumping a $k = 0$ magnons first and letting the system go through a three-magnon interaction to generate the $\pm k$ magnon pair. The latter one is known as perpendicular pumping in microwave excitation of magnons [39].

There are also two mechanisms to form mBEC after pumping. One is that magnons are gradually scattered from the pumping frequency to the bottom of the spectrum through a cascade process [9,26]. The other one is through the kinetic instability (KI) process where the pumped magnons are directly scattered into state near the bottom of the spectrum [27,28]. The theoretical explanation for the cascade process was proposed by Rezende [29], whereas the theoretical model for KI process presented here was introduced in our study. Altogether, we have four paths towards mBEC in an optical cavity. In the following subsections, we will check the possibility of the four procedures one by one.

C. Direct pumping and mBEC in cavity

Šimić *et al.* [24] have shown that a large number of coherent magnons at a selected mode can be excited in a YIG sphere with two counterpropagating optical modes, similar to stimulated-Raman scattering. Here, we apply their theory to an optomagnonic cavity and generalize it to the excitation of a magnon pair with opposite wave vectors in a YIG waveguide. Figure 1(c) demonstrates the four laser beams applied to the cavity. Lasers with “ \pm ” subscripts are used to pump the $\pm k$ -magnon modes. For example, we need a TE light and a TM light, which are blue detuned to the cavity mode and satisfy $\omega_{TE} < \omega_{TM}$ to excite the $-k$ magnon mode.

In the direct pumping process, due to the different coupling strengths of the $+k$ and $-k$ magnons as shown in Sec. III, it is necessary to adjust the laser powers $P^{(+)}$ and $P^{(-)}$ to produce an equal number of $+k$ and $-k$ magnons according to Eq. (2). Here, we assume that the equal number is n .

1. Cascade process

We will discuss the formation of mBEC through the cascade process first. In direct pumping, the total number of pumped magnons is

$$N_p = 2n, \quad (6)$$

where n is determined by Eq. (2). After preparation of a large number of magnons in $\pm k$ state far out of thermal equilibrium, the laser beams can be switched off and the four-magnon interaction will redistribute these pumped magnons to other energy states in the range $[\omega_{k_0}, \omega_k]$. The redistribution process is the same as that for parallel pumping by microwave pulses, which has been discussed in detail by Rezende in Ref. [29]. We will apply Rezende’s result of critical magnon number to derive the threshold power of input lasers in our system.

The redistributed magnons are in quasiequilibrium state and have a temperature higher than the environment, which are called reservoir magnons. The critical number of magnons pumped into the reservoir should be

$$n_{D,c1} = \frac{2N_R}{f_4 G(\omega_{k_0})}, \quad (7)$$

where the subscript D stands for direct pumping and c_1 for the critical value through the cascade process, N_R is the total mode number of magnons in the reservoir, $f_4 = 4\omega_M/(NS)$ is the interaction coefficients with $\omega_M = \gamma M = 3 \times 10^{10}$ Hz and NS the total spin in the film [40], and $G(\omega_{k_0})$ is the density of spectrum at the bottom of the spectrum normalized weighted by the normalized Bose-Einstein distribution,

$$G(\omega) = \frac{D(\omega)n_{BE}(\omega)}{\frac{1}{\Delta\omega_k} \int n_{BE}(\omega)d\omega}, \quad (8)$$

with $D(\omega)$ being the density of states of magnons, $n_{BE}(\omega)$ the Bose-Einstein distribution, and $\Delta\omega_k$ the frequency range of the reservoir magnons. We have checked the critical magnon number using the parameters obtained from the experiments conducted by Demidov *et al.* [41]. The resulting number is 0.9×10^{16} , in good agreement with that converted from the threshold power measured in the conventional microwave pumping experiments, affirming the reliability of the theoretical model.

Combing Eq. (7) with Eq. (2), we obtain the threshold power required for the formation of mBEC by direct pumping in an optical cavity through the cascade process, which is

$$P_{D,c1} = \left(\frac{2N_R}{f_4 G(\omega_{k_0})} \right)^{1/2} \frac{\hbar\kappa_m \omega_{opt} \kappa_{opt}}{2|g_k|}. \quad (9)$$

Above this threshold, the reservoir magnons can be divided into two categories: one in quasiequilibrium obeying Bose-Einstein distribution; the other one contains a larger number of magnons and has frequencies in the vicinity of the lowest frequency k_0 , which forms the mBEC.

2. KI process

We consider now the large number of magnons in $\pm k$ states pumped into cavity system that do not go through a cascade redistribution but undergo a KI process via four-magnon interactions instead. Although there has been experimental demonstration of the KI process in the formation of mBEC by microwave pumping, a significant gap remains in theoretical predictions regarding the threshold powers necessary for this process to occur. In this subsection, we address this gap by constructing a comprehensive theoretical model based on four-magnon interactions. Our model not only clarifies the fundamental mechanisms driving the KI process but also offers a predictive framework for estimating the threshold powers required to initiate mBEC formation through this pathway.

In the KI process, a portion of the $\pm k$ magnons are scattered to the bottom of the spectrum at $(\omega_{k_0}, \pm \mathbf{k}_0)$ while the rest of them to the higher-energy states $(\omega_{k_1}, \mathbf{k}_1)$ that hold energy and momentum conservation,

$$\begin{aligned}\omega_k + \omega_k &= \omega_{k_0} + \omega_{k_0}, \\ \mathbf{k} + \mathbf{k} &= \mathbf{k}_0 + \mathbf{k}_1.\end{aligned}\quad (10)$$

To provide an illustration of the KI process in phase space, we need to know the dispersion relation of magnon [29]

$$\omega_k^2 = \gamma^2 [H_y + Dk^2 + M(1 - F_k)\sin^2\theta_k][H_y + Dk^2 + MF_k] \quad (11)$$

with

$$F_k = (1 - e^{-kd})/|k|d, \quad (12)$$

where $k^2 = k_x^2 + k_y^2$ is the magnon wave vector in plane, $\gamma = g\mu_B/\hbar$ is the gyromagnetic, $D = \frac{2JSa^2}{g\mu_B\mu_0}$ is the exchange parameter, M is the magnetization of the material, and θ is the angle between the 2D wave vector \mathbf{k} and the direction of static magnetic field H_y . The competition between the dipolar interaction and exchange interaction leads to a magnon spectrum ω_k with two minima located at $\pm k_0$ in 2D wave-vector space. The YIG waveguide studied in our proposal has a length of $l = 8000 \mu\text{m}$ and a cross section of $2w \times d = 400 \times 4 \mu\text{m}^2$. In this case, only the wave vector along the length direction k_y can be seen as continuous, and k_x becomes discrete as $k_x = \frac{n\pi}{2w}$, where $n = 1, 3, 5, 7, 9, \dots$, is the mode index of magnons that can be excited in the waveguide under pinned boundary conditions [42,43].

Figure 2 illustrates the KI process in k space where the purple line represents the isofrequency surfaces with $\omega_k = 4$ GHz, the red dot locates k_0 with the minimal energy $\omega_{k_0} = 2.51$ GHz, and the orange line represents the isofrequency surfaces with $\omega_{k_1} = 2\omega_k - \omega_{k_0} = 5.49$ GHz. The green dots denote the magnon modes that can be scattered to $(\omega_{k_0}, \mathbf{k}_0)$ state via the KI process at given frequency ω_k .

The Hamiltonian of the KI process can be written as

$$H^{(4)} = \hbar \sum_k \hbar f_4 b_k b_k^\dagger b_{k_0}^\dagger b_{k_1}^\dagger + \text{H.c.}, \quad (13)$$

where $\mathbf{k}_1 = 2\mathbf{k} - \mathbf{k}_0$, and f_4 is the same four-magnon interaction coefficient as shown in Eq. (7).

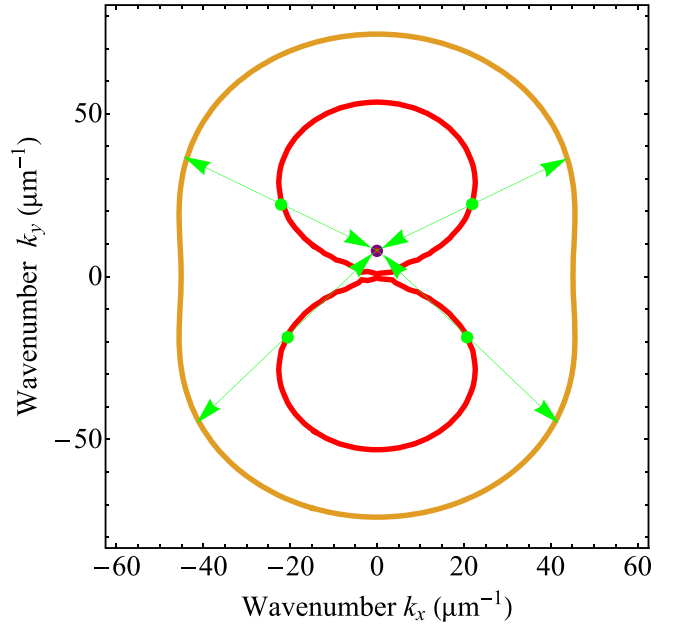


FIG. 2. Illustration of the KI process for $H_y = 0.858$ Oe, $\gamma = 2.8$ GHz/kOe, $M = 1.76$ kG, and $D = 2 \times 10^9$ Oe cm^2 . The purple dot is the minimal energy with $\omega_{k_0} = 2.51$ GHz. The red and orange lines represent the isofrequency surfaces of $\omega_k = 4$ GHz and $\omega_{k_1} = 5.49$ GHz, respectively; the green dots denote the modes for which the KI process can occur. The green arrows illustrate the KI process.

In analogy to the second Shul process [39], we treat the magnon operator b_k , which is initially pumped into the system, as a classical variable. Consequently, the four-magnon interactions can be expressed as

$$H^{(4)} = H_{\text{eff}} = \sum_k \hbar \rho_k e^{-2i\omega_k t} b_{k_0}^\dagger b_{k_1}^\dagger + \text{H.c.}, \quad (14)$$

where $\hbar \rho_k = f_4 |b_k|^2 = f_4 N_p$. Combining with the Hamiltonian of free magnons

$$H_0 = \hbar \sum_k \omega_k b_k^\dagger b_k, \quad (15)$$

we can get the equation of motion of b_{k_0} and b_{k_1} ,

$$\begin{aligned}\frac{db_{k_0}}{dt} &= -(i\omega_{k_0} + \eta_{k_0})b_{k_0} - i\hbar \rho_k e^{-2i\omega_k t} b_{k_1}^\dagger, \\ \frac{db_{k_1}}{dt} &= -(-i\omega_{k_0} + \eta_{k_1})b_{k_1} + i\hbar \rho_k e^{-2i\omega_k t} b_{k_0}.\end{aligned}\quad (16)$$

where η_{k_i} is the magnon damping rate of k_0 and k_1 . Introducing the slowly varying spin-wave amplitude $\tilde{b}_{k_i} = \langle b_{k_i} \rangle e^{i\omega_{k_i} t}$ [39] with $i = 0, 1$, we can obtain

$$\begin{aligned}\frac{d\tilde{b}_{k_0}}{dt} &= -(i\Delta\omega_{k_0} + \eta_{k_0})\tilde{b}_{k_0} - i\hbar \rho_k \tilde{b}_{k_1}^*, \\ \frac{d\tilde{b}_{k_1}^*}{dt} &= -(-i\Delta\omega_{k_1} + \eta_{k_1})\tilde{b}_{k_1}^* + i\hbar \rho_k \tilde{b}_{k_0},\end{aligned}\quad (17)$$

where $\Delta\omega_{k_i} = \omega_{k_i} - \omega_k$ and $\Delta\omega_{k_1} = \Delta\omega_{k_0}$. The above equation have solutions of the form $\tilde{b}_{k_0} \propto \exp(\gamma_k t)$. Then it is easy

to show that the two eigenvalues correspond to

$$\gamma_k = -\frac{1}{2}(\eta_{k_0} + \eta_{k_1}) \pm \frac{1}{2}[(\eta_{k_0} + \eta_{k_1})^2 - 4\eta_{k_0}\eta_{k_1} + 4(h^2\rho_k^2 - \Delta\omega_k^2)]^{1/2}. \quad (18)$$

The spin wave instability occurs when $\gamma_k > 0$ (the eigenvalue with the upper sign), which makes magnon number grow exponentially in time, and gives the threshold pumping parameter

$$(h\rho_k)_c = [\eta_{k_0}\eta_{k_1} + (\Delta\omega_k)^2]^{1/2}. \quad (19)$$

In magnon system, we assume that the relaxation rates are the same for different modes $\eta_{k_0} = \eta_{k_1} = \eta_m$. And $h\rho_k = f_4 N_p = 2f_4 n$ is directly related to the pumped magnon number, so the critical number of $\pm k$ magnon can be written as

$$n_{D,c2} = \frac{[\eta_m^2 + (\Delta\omega_k)^2]^{1/2}}{2f_4}. \quad (20)$$

The corresponding threshold laser power is

$$P_{D,c2} = \left(\frac{[\eta_m^2 + (\Delta\omega_k)^2]^{1/2}}{2f_4} \right)^{1/2} \frac{\hbar\kappa_m\omega_{\text{opt}}\kappa_{\text{opt}}}{2|g_k|}. \quad (21)$$

Notice that the critical number is related to the frequency difference $\Delta\omega_k$. The larger the difference is, the more pumped magnons are in need. The coherent properties of KI-mBEC will be proved in Appendix B using the methods of statistical mechanics appropriate for bosonic systems interacting with a heat bath [29,44].

D. Perpendicular pumping in cavity

Based on the first Shul process [39,40], the $k = 0$ magnon can also split into a pair of $\pm k$ magnons, which is crucial for stabilizing mBEC. The splitting can be described by a three-magnon interaction induced by the magnetic dipolar interaction,

$$H^{(3)} = \frac{\hbar}{2} \sum_k f_3 b_0 b_k^\dagger b_{-k}^\dagger + \text{H.c.}, \quad (22)$$

where

$$f_3 = -\frac{\omega_M}{\sqrt{2SN}} \sin 2\theta_k e^{i\varphi_k}, \quad (23)$$

is the three-magnon interaction coefficient [40]. Similar to the KI process, we can transform $H^{(3)}$ into an effective field that pumps $\pm k$ magnons,

$$H^{(3)} = H'_{\text{eff}} = \frac{\hbar}{2} \sum_k (h\rho_k)_{\text{eff}} e^{-i\omega_0 t} b_k^\dagger b_{-k}^\dagger + \text{H.c.}, \quad (24)$$

where $(h\rho_k)_{\text{eff}} = \sqrt{n_0} f_3$ is the effective field. For $\omega_0 = 2\omega_k$, i.e., when $\Delta\omega_k = 0$, the critical number of magnons occurring in this process is given by

$$n_c = (\eta_m/|f_3|)^2, \quad (25)$$

where η_m is the magnon-magnon relaxation rate. Above this critical number, the number of magnons in the k state with $\omega_k = \omega_0/2$ is increased and achieves a steady state via the

four-magnon interaction as in [39]. The average magnon number in the steady k state is

$$N_{P,p} = \langle n_k \rangle = \frac{[(n - n_c)/n_c]^{1/2}}{2f_4/\eta_m}, \quad (26)$$

where n is the magnon number for $k = 0$. The following treatment of achieving mBEC is the same as that for direct pumping with replacing N_p by $N_{P,p}$ in $h\rho_k$. Here we give the final results only. For the cascade process, the critical pumped magnon number is

$$n_{P,c1} = n_c \left\{ 1 + \frac{16N_R}{[\eta_m G(\omega_{k_0})]^2} \right\}, \quad (27)$$

and the threshold power is

$$P_{P,c1} = \left(1 + \frac{16N_R}{[\eta_m G(\omega_{k_0})]^2} \right)^{1/2} \frac{\hbar\kappa_m\eta_m\omega_{\text{opt}}\kappa_{\text{opt}}}{2|g_k|f_3}. \quad (28)$$

For the KI process, the critical pumped magnon number is

$$n_{P,c2} = n_c [5 + (\Delta\omega_k/\eta_m)^2], \quad (29)$$

and the threshold power is

$$P_{P,c2} = [5 + (\Delta\omega_k/\eta_m)^2]^{1/2} \frac{\hbar\eta_m\kappa_m\omega_{\text{opt}}\kappa_{\text{opt}}}{2|g_k|f_3}. \quad (30)$$

III. NUMERICAL RESULTS

Up to now, we have introduced two ways to pump $\pm k$ magnons and two mechanisms to generate mBEC after pumping within an optical cavity. In this section, we will calculate the critical magnon number and the threshold laser power for the formation of mBEC with realistic parameters to check the feasibility of our proposal.

In YIG waveguide, the lattice constant $a = 1.23$ nm, and the net spin per formula unit is $S = 5/2$, so we obtain $NS = 1.72 \times 10^{16}$, $f_3 = 162$ Hz, $f_4 = 7 \times 10^{-6}$ Hz, and $G(\omega_{k_0})/N_R = 9.5 \times 10^{-10}$ Hz⁻¹ in our model. The magnon-magnon damping rate $\eta_m = 5 \times 10^7$ Hz as in [29]. κ_m is related to the Gilbert damping. We use the same parameter $\alpha = 3 \times 10^{-5}$ as in [25] and obtain $\kappa_m = \alpha\omega_k = 0.12$ MHz. The optical damping rate is taken $\kappa_{\text{opt}} = 35$ MHz as in [23].

We begin by focusing on the magnon-photon coupling strength (g_k) to access whether a specific magnon mode can be coherently pumped by light in the cavity. Detailed calculations are presented in Appendix A. Figure 3 gives $|g_k|$ as a function of magnon wave vector for a given frequency (4 GHz in the figure). The results exhibit apparent nonreciprocity between $+k$ and k magnons. The red dots represent one of the magnon pairs that can be excited within the cavity using the direct pumping approach. Notably, the corresponding wave vectors of these dots are $-0.09 \mu\text{m}^{-1}$ and $+0.1 \mu\text{m}^{-1}$, respectively, which are not exactly symmetric around zero due to momentum conservation imposed by the magnon-photon interaction. However, considering a magnon linewidth of $\eta_m = 50$ MHz at $\omega = 4$ GHz, the wave-vector errors fall in the range of $[0.073, 0.108] \mu\text{m}^{-1}$. Consequently, it is reasonable to regard them as a $\pm k$ pair. In contrast, the $k = 0$ magnon cannot be excited in the optical cavity under examination due to mode mismatch. In other words, the perpendicular pumping scenario cannot be realized within the rectangular waveguide

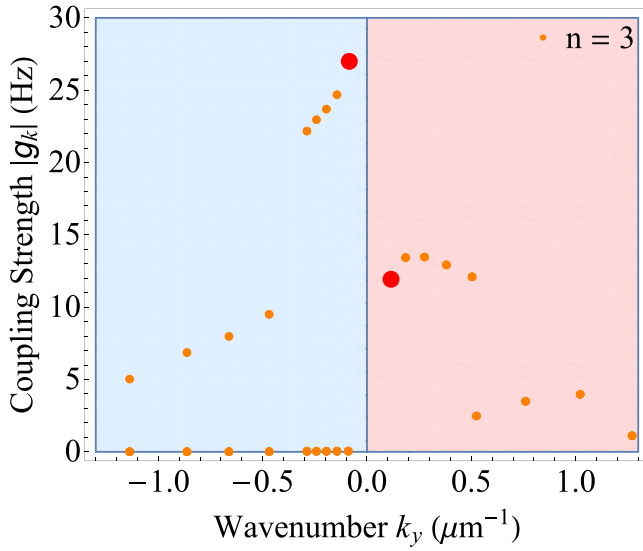


FIG. 3. The intrinsic magnon-photon coupling strength as a function of magnon wave vectors for different incident and scattered light modes calculated from Eq. (A3) for the magnon width mode $n = 3$ in an optical cavity. The blue (pink) area on the left (right) represents the Stokes process for the $-k(+k)$ magnons. The excited $-k$ magnon has a maximum coupling strength of 27 Hz at $k = -0.09 \mu\text{m}^{-1}$, represented by the red point in the blue area, while the excited $+k$ magnon has a coupling strength of 12 Hz at $k = 0.1 \mu\text{m}^{-1}$, represented by the red point in the pink area.

considered here. Henceforth, all subsequent discussions are based on the direct pumping process.

For cascade process after direct pumping, we obtain the critical number $N_{D,c1} = 5.51 \times 10^{14}$ using Eqs. (7) and (9). Because of the nonreciprocity we need two threshold powers to pump the $\pm k$ magnons up to the same critical number. We denote the pumping power for $+k$ and $-k$ magnons as $P^{(+)}$ and $P^{(-)}$, respectively, for different coupling strength in Appendix A. The corresponding power is $P_{D,c1}^{(+)} = 87.8$ mW, $P_{D,c1}^{(-)} = 37.6$ mW.

For the KI process, the critical number for the formation of BEC depends on the values of $\Delta\omega_k$, when $\Delta\omega_k = 1.49$ GHz, we can obtain $n_{D,c2} = 1.06 \times 10^{14}$ using Eq. (21). The resulting laser power is shown in Table I. The critical powers of these two processes are very close, they are intended to take place simultaneously by the direct pumping method if the magnon modes localize at the KI points. As discussed in Sec. II C, magnons have to be pumped in specific modes (the green points for example) to launch the KI process. Therefore, one can turn off the KI process and initiate the cascade process only by adjusting the applied magnetic field

TABLE I. Critical magnon number and threshold laser power for mBEC in direct pumping for different mechanism.

Critical value	Cascade (D, c1)	KI (D, c2)
$n (\times 10^{14})$	5.51	1.06
$P^{(+)}(\text{mW})$	87.8	38.4
$P^{(-)}(\text{mW})$	37.6	16.8

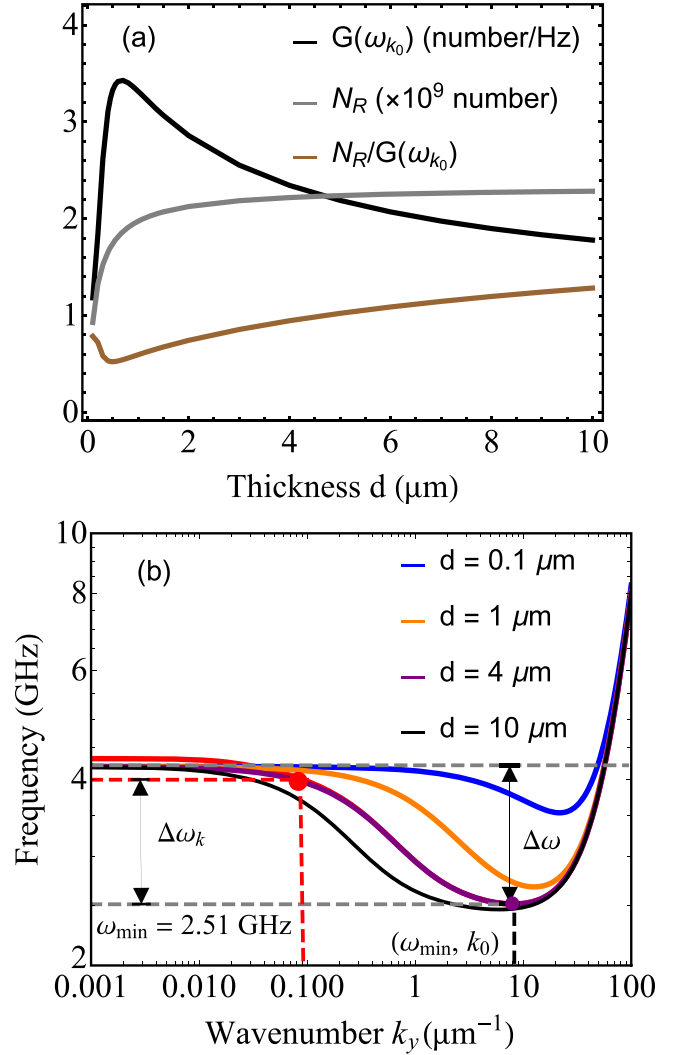


FIG. 4. (a) The dependence of $G(\omega_{k_0})$ and N_R on the thickness d . (b) The effect of thickness on $n = 0$ mode, here $\Delta\omega_k$ is the frequency between pumped magnon ω_k and lowest energy magnon ω_{\min} , the red line represent $n = 3$ mode for $d = 4 \mu\text{m}^{-1}$, and the red dot represent $n = 3$ mode pumped into YIG film by laser.

to tune the pumped magnons away from satisfying the energy-momentum conservations. In this way, the two mechanisms of generating mBEC in an optical cavity can be examined separately in experiments.

Furthermore, upon comparing the expressions [Eqs. (9) and (21)] for the threshold powers of the cascade and KI processes after direct pumping, we discovered that the waveguide thickness plays a crucial role in determining these threshold powers. Specifically, for the cascade process threshold power ($P_{D,c1}$), both $G(\omega_{k_0})$ and N_R are intricately linked to the density of states of magnons, a quantity directly influenced by the waveguide thickness, as illustrated in Fig. 4(a). Notably, the total number of modes in the magnon reservoir (depicted by the gray line) increases monotonously with increasing thickness, whereas the spectral density $G(\omega_{k_0})$ (shown by the black line) initially rises and then declines with thickness, reaching a peak at $d = 0.5 \mu\text{m}$. However, the net effect of thickness on $P_{D,c1}$ hinges on the ratio $G(\omega_{k_0})/N_R$ (depicted by

the brown line), which remains relatively stable across varying thicknesses. Conversely, for the KI process following direct pumping, the threshold power's magnitude strongly correlates with $\Delta\omega_k$, which decreases monotonously as the waveguide thickness decreases [Fig. 4(b)]. As per Eq. (21), a smaller $\Delta\omega_k$ translates to a lower $P_{D,c2}$. As a result, the KI process is more likely to predominate over the cascade process in thinner waveguides.

IV. CONCLUSIONS

In conclusion, we propose a platform to generate Bose-Einstein condensation of magnons, which is in an optomagnonic waveguide. In order to stabilize the obtained mBEC, pumping of $\pm k$ -magnon pairs is required. In an optical cavity composed of a ferromagnetic insulator, magnons of selected wave vector can be pumped coherently by two optical cavity modes through stimulated-Raman-like scattering. Due to the extremely low coupling strength between the $k = 0$ magnon and the cavity photons, an indirect optical pumping method through three-magnon splitting is ruled out. But a direct pumping of $\pm k$ -magnon pairs is proved to be realistic. Based on the selection rule of the optomagnonic waveguide, this can be achieved by applying four input lasers with powers less than 1 watt, two of which are blue detuned and polarized along the TM and TE modes, respectively. The other two lasers should be red detuned with inverse polarizations. Both the cascade and the KI processes toward mBEC are possible after the coherent pumping of magnon pairs, with the KI process predominant in thinner waveguides. However, one can switch off the KI process by adjusting the applied magnetic field. The realization of this optically driven mBEC will add new options to genuine quantum magnonics.

ACKNOWLEDGMENTS

This work was financially supported by the National Natural Science Foundation of China (Grant No. 11904256) and the National Key R&D Program of China (Grant No. 2021YFF1200700).

APPENDIX A: COUPLING STRENGTH

In a hybrid quantum system consisting of an optical cavity and a magnetic YIG film, the total Hamiltonian of the system can be expressed as

$$H = H_0 + H_1, \quad (\text{A1})$$

where $H_0 = \sum_q \hbar\omega_q a_q^\dagger a_q + \sum_k \hbar\omega_k b_k^\dagger b_k$ is the noninteracting Hamiltonian. The modes of incident and scattered light in an optical cavity are denoted by m and m' , respectively, and q is the wave vectors of photon. The magnon modes are represented by width mode index n and wave vector k . H_1 stands for the magnon-photon interaction,

$$H_1 = \sum_{m,m',k_n} [\hbar g_{mm'n}^{(+)} a_m a_{m'}^\dagger b_{k_n} \delta(q_m - q_{m'} + k_n) + \hbar g_{mm'n}^{(-)} a_m a_{m'}^\dagger b_{k_n}^\dagger \delta(q_m - q_{m'} - k_n)], \quad (\text{A2})$$

where $g_{mm'n}^{(\pm)}$ is the coupling strength

$$g_{mm'n}^{(\pm)} = \left(\frac{2\hbar\gamma}{M_0V} \right)^{\frac{1}{2}} \frac{c_0}{n_0^2} [\Phi_{\text{MLB}} G_{44,mm'n}^{(\pm)} \pm \Phi_{\text{MCB}} K_{mm'n}^{(\pm)}]. \quad (\text{A3})$$

Φ_{MLB} and Φ_{MCB} represent the magnetic circular birefringence and magnetic linear birefringence, respectively. The overlap integration is shown to be

$$G_{44,mm'n}^{(\pm)} = \frac{1}{S} \int_{-w}^w d\xi \int_{-d}^d d\zeta (e_{1m,z}^* e_{2m',x} \mp i e_{1m,z}^* e_{2m',y} + e_{1m,x}^* e_{2m',z} \mp i e_{1m,y}^* e_{2m',z}) \phi_n(\xi, \zeta), \\ K_{mm'n}^{(\pm)} = \frac{1}{S} \int_{-w}^w d\xi \int_{-d}^d d\zeta (e_{1m,z}^* e_{2m',x} \mp i e_{1m,z}^* e_{2m',y} - e_{1m,x}^* e_{2m',z} \pm i e_{1m,y}^* e_{2m',z}) \phi_n(\xi, \zeta), \quad (\text{A4})$$

where $S = 4wd$ is the area of the film cross section, $e_{\alpha m}(\xi, \zeta)$ is the normalized field function of the different modes in the optical cavity. Because the thickness is much smaller than the width, we can consider that the magnon mode wave function along thickness direction is homogeneous, so the wave function of magnon is only related to the width direction, namely

$$\phi_n(\xi, \zeta) = \cos\left(\frac{n\pi\xi}{2w}\right), \quad (\text{A5})$$

where $n = 1, 3, 5, 7, 9, \dots$ and w is the half width of the film. From the above expressions, it can be seen that the magnitude of the coupling strength $g_{mm'n}^{(\pm)}$ primarily depends on the overlap integral between the cavity mode and the magnon mode.

In cavity optomagnonics system, a pronounced non-reciprocity and asymmetry exist in Stokes process and anti-Stokes process, which $g^{(+)}$ is strongly suppressed in Stokes process and $g^{(-)}$ is suppressed in anti-Stokes process [30]. So we only calculate the coupling strength $g_{mm'n}^{(-)}$ in the Stokes process. We choose an incident photon with a wavelength of $1.55 \mu\text{m}$ to excite the magnons with a frequency of 4 GHz. The calculation results show that the maximum coupling strength $g^{(-)} \approx 2\pi \times 27 \text{ Hz}$ can be obtained when the incident light is TE_{00} and the scattered light is TM_{31} ($\text{TE}_{00} \rightarrow \text{TM}_{31} + \phi_3$), and the magnon mode is $n = 3$, with the corresponding magnon wave vector $k_y = -0.09 \mu\text{m}^{-1}$ as shown in Fig. 3. By adjusting the external magnetic field applied to the YIG film to $H_y = 858 \text{ Oe}$, the excited magnons in the cavity can be precisely located on the magnon spectrum with $n = 3$. As for the minimal wave vector of $+k$ magnon is taken $k_y = -0.1 \mu\text{m}^{-1}$ with $g^{(-)} \approx 2\pi \times 12 \text{ Hz}$, corresponding to $\text{TM}_{00} \rightarrow \phi_3 + \text{TE}_{11}$. We also observed that when $n > 11$, the coupling strength decreases to almost zero, which means that it is unable to pump magnons of higher width mode, and the modes that can be pumped in cavity are illustrate in Fig. 5 for orange line. The reason is that as n increases, the volume wave gradually change to surface wave, resulting in a significant reduction in the overlap integral and thus a decrease in the corresponding coupling strength, which has also been verified through experiments [44].

We also studied the relationship between the magnon wave vector and the corresponding coupling strength in the cavity when the incident light is TE and the scattered light is TM. For

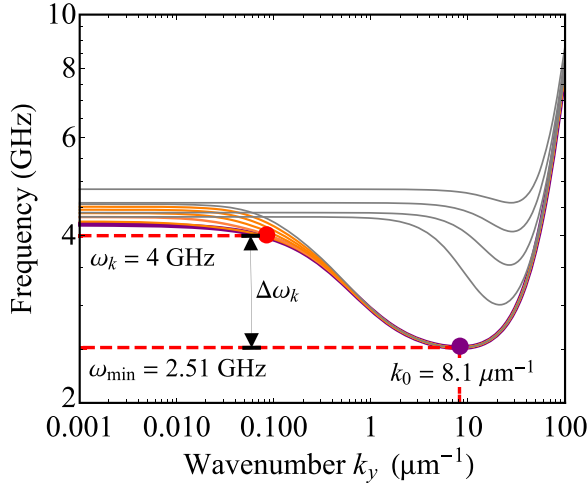


FIG. 5. Different width modes for $d = 4 \mu\text{m}$, where the purple line represent $n = 0$, which is the lowest energy mode, the orange lines for $n = 1, 3, 5, 7, 9$, and the gray lines for much higher mode n . The red dot represents $n = 3$ mode pumped into YIG film by laser.

a thickness of $2d = 4 \mu\text{m}^{-1}$, the lower limit of the magnon wave vector that can be excited in the cavity is $0.09 \mu\text{m}^{-1}$, and the upper limit is $1.27 \mu\text{m}^{-1}$. The excitation of magnons in the cavity is determined by the energy and the momentum conservations between photons and magnons. Since the optical photon frequency is generally in the order of hundreds of terahertz, while the magnon frequency is in the order of gigahertz, the momentum difference between the incident and scattered photons is actually very small. This leads to the magnon momentum excited in the optical cavity being confined to a relatively small range, typically only in the dipolar part of the magnon.

We found that the magnons that can be excited in the film also depend on the thickness of the film. Under the same conditions, the thinner the film, the fewer magnon modes can be excited in the cavity, and the larger the spacing between different modes. In such cases, the lower bound of the magnon wave vector that can be excited is further away from long-wavelength limit. Due to the limitation of the lower limit of magnon wave vectors that can be generated in the cavity, we cannot pump magnons with $k = 0$, which makes perpendicular pumping impractical in the cavity. Only the direct pumping can be used to generate magnons, and the wave vector in the width direction of the pumped magnons is almost zero. The magnons pumped by the cavity are all located in the y direction.

APPENDIX B: COHERENT PROPERTY OF MBEC

The coherence of k_0 magnon in the bottom of the spectrum can be demonstrated by the statistical mechanics appropriate for bosonic systems interacting with a heat bath. We follow the same procedure used by de Araujo [45]. The cascade process has been demonstrated in [29]. Here, we only study the KI process.

Under the consideration of heat bath the total Hamiltonian of the systems can be expressed as follows:

$$\begin{aligned}
 H &= H_0 + H^{(4)} + H_{\text{eff}}(t) + H_R + H_{RS}, \\
 H_0 &= \hbar \sum_{k_1} \omega_k b_k^\dagger b_k, \\
 H_{\text{eff}} &= \hbar \sum_k h \rho_k e^{-2i\omega_k t} b_{k_0}^\dagger b_{k_1}^\dagger + \text{H.c.}, \\
 H^{(4)} &= f_4 \sum_{k_2, k_3} b_{k_0+k_2} b_{k_0-k_2} b_{k_0+k_3}^\dagger b_{k_0-k_3}^\dagger. \quad (\text{B1})
 \end{aligned}$$

The four-magnon interactions take place near k_0 state, H_{eff} is the effective Hamiltonian that excites the k_0 magnon in the KI process. H_R is the Hamiltonian for the magnon reservoir, assumed to be a system with large thermal capacity and in thermal equilibrium. H_{RS} represents a linear interaction between the magnon system and the heat reservoir,

$$\begin{aligned}
 H_R &= \hbar \sum_R \omega_R B_R^\dagger B_R, \\
 H_{RS} &= \hbar \sum_{k,R} \beta_{k,R}^* B_R^\dagger b_k + \beta_{k,R} B_R b_k^\dagger. \quad (\text{B2})
 \end{aligned}$$

The equations of motion of b_{k_0} and b_{k_1} can be obtained by using the Heisenberg equation

$$\begin{aligned}
 \frac{db_{k_0}}{dt} &= -(i\omega_{k_0} + \eta_{k_0} + i f_4 n_{k_0}) b_{k_0} - i h \rho_k e^{-2i\omega_k t} b_{k_1}^\dagger + F_{k_0}(t), \\
 \frac{db_{k_1}^\dagger}{dt} &= -(i\omega_{k_1} + \eta_{k_1} + i f_4 n_{k_1}) b_{k_1}^\dagger - i h \rho_k e^{-2i\omega_k t} b_{k_0} + F_{k_1}^*(t), \quad (\text{B3})
 \end{aligned}$$

where

$$F_{k_0}(t) = -i \sum_R \beta_{k_0,R} B_R e^{-i\omega_R t} \quad (\text{B4})$$

is the Langevin random force of Markoffian systems. Transforming Eq. (B3) to the representation of coherent state $|\alpha_k\rangle$, and working with variables in a rotating wave frame $b_k |\alpha_k\rangle = \alpha_k(t) e^{-i\omega_k t} |\alpha_k\rangle$, we obtain an equation of motion for the coherent state,

$$\begin{aligned}
 \frac{d\alpha_{k_0}}{dt} &= -(\eta_{k_0} + i f_4 n_{k_0}) \alpha_{k_0} - i h \rho_k e^{-2i(\omega_k - \omega_{k_0})t} \alpha_{k_1}^* \\
 &\quad + F_{k_0}(t) e^{i\omega_{k_0} t}, \quad (\text{B5a})
 \end{aligned}$$

$$\begin{aligned}
 \frac{d\alpha_{k_1}^*}{dt} &= -(\eta_{k_1} - i f_4 n_{k_1}) \alpha_{k_1}^* + i h \rho_k e^{2i(\omega_k - \omega_{k_1})t} \alpha_{k_0} \\
 &\quad + F_{k_1}^*(t) e^{-i\omega_{k_1} t}. \quad (\text{B5b})
 \end{aligned}$$

Assuming that $n_{k_0} = n_{k_1} = |\alpha_{k_0}|^2$ and after some manipulation we obtain

$$\begin{aligned}
 \frac{d\alpha_{k_0}}{dt} - \frac{(f_4)^2}{\eta_{k_1}} \left[\frac{(h\rho_k)^2 - \eta_{k_0} \eta_{k_1}}{(f_4)^2} - |\alpha_{k_0}|^4 \right] \alpha_{k_0} &= S_k, \\
 S_k &= -i \frac{h\rho_k}{\eta_{k_1}} F_{k_1}^*(t) e^{-i\Omega_1 t} + F_{k_0}(t) e^{i\omega_{k_0} t}, \quad (\text{B6})
 \end{aligned}$$

where $\Omega_1 = 2\omega_k - 2\omega_{k_0} + \omega_{k_1}$. Equation (B6) is a typical nonlinear Langevin equation that appears in Brownian motion studies and laser theory. It shows that the magnon modes with

amplitude k are driven thermally by the hot magnon reservoir and also by an effective driving field. Using $\alpha_{k_0} = r_{k_0} e^{i\phi_{k_0}}$, the corresponding Fokker-Planck equation of Eq. (B6) is

$$\begin{aligned} \frac{\partial P}{\partial t} + \beta \frac{1}{r_{k_0}} \frac{\partial}{\partial r_{k_0}} [(n - r_{k_0}^4) r_{k_0}^2 P] \\ = Q \left(\frac{1}{r_{k_0}} \frac{\partial}{\partial r_{k_0}} r_{k_0} \frac{\partial P}{\partial r_{k_0}} + \frac{1}{r_{k_0}^2} \frac{\partial^2 P}{\partial \phi_{k_0}^2} \right), \end{aligned} \quad (\text{B7})$$

where $\beta = \frac{(f_4)^2}{\eta_{k_1}}$, $m = \frac{(h\rho_k)^2 - \eta_{k_0}\eta_{k_1}}{(f_4)^2}$ and

$$\begin{aligned} Q &= \frac{1}{T} \int_0^T \int_0^T \langle S_k(t_1) S_k^*(t_2) \rangle dt_1 dt_2 \\ &= \eta_{k_0} (\bar{n}(\omega_{k_0}) + 1) + \eta_{k_{\Omega_1}} \frac{(h\rho_k)^2}{\eta_{k_1}} \bar{n}(\Omega_1) \end{aligned} \quad (\text{B8})$$

is calculated in [46]. The normalized Fokker-Planck equation can be obtained by dividing $(\beta Q)^{1/3}$ on both sides

$$\frac{\partial P}{\partial t'} + \frac{1}{x} \frac{\partial}{\partial x} [(A - x^4) x^2 P] = \frac{1}{x} \frac{\partial}{\partial x} \left(x \frac{\partial P}{\partial x} \right) + \frac{1}{x^2} \frac{\partial^2 P}{\partial \phi_{k_0}^2}, \quad (\text{B9})$$

where

$$t' = (\beta Q)^{1/3} t, \quad x = \left(\frac{\beta}{Q} \right)^{1/6} r_{k_0}, \quad A = \left(\frac{\beta}{Q} \right)^{2/3} m, \quad (\text{B10})$$

represent normalized parameters. Here we are interested only in the stationary solution of Eq. (B9), that is, the equation is independent of ϕ_{k_0} . Straightforward integration gives

$$P(x) = C \exp\left(\frac{1}{2} A x^2 - \frac{1}{6} x^6\right), \quad (\text{B11})$$

where C is a normalization constant, the integral of Eq. (B11) from $x = 0$ to infinity is equal to 1. The parameter A in the equation corresponds to different distributions of P . When $A < 0$, $P(x)$ represents a Gaussian distribution describing incoherent magnons at thermal equilibrium. When $A > 0$, $P(x)$ describes a state composed of both coherent and incoherent magnons. When $A \gg 1$, $P(x)$ represents a delta function distribution, describing coherent magnons. The parameter A is mainly decided by m , in the case of $(h\rho_k)^2 > \eta_{k_1}\eta_{k_0}$, $m > 0$, and the condition of the KI process happened is $(h\rho_k)^2 > \eta_{k_1}\eta_{k_0} + (\Delta\omega_{k_0})^2$, so we can draw a conclusion that the k_0 magnon generated by KI process is coherent state. The coherent property of $k = 0$ magnon BEC can also be demonstrated using the same way.

-
- [1] Bose, Plancks Gesetz und Lichtquantenhypothese, *Z. Phys.* **26**, 178 (1924).
- [2] A. Einstein, Quantentheorie des einatomigen idealen Gases. Part I. Sber. Preuss. Akad. Wiss. **22**, 261 (1924); Quantentheorie des einatomigen idealen Gases. Part II. Sber. Preuss. Akad. Wiss. **1**, 3 (1925).
- [3] J. F. Allen and A. D. Misener, Flow of liquid helium II, *Nature (London)* **141**, 75 (1938).
- [4] M. H. Anderson, J. R. Ensher, M. R. Matthews, C. E. Wieman, and E. A. Cornell, Observation of Bose-Einstein condensation in a dilute atomic vapor, *Science* **269**, 198 (1995).
- [5] D. G. Fried, T. C. Killian, L. Willmann, D. Landhuis, S. C. Moss, D. Kleppner, and T. J. Greytak, Bose-Einstein condensation of atomic hydrogen, *Phys. Rev. Lett.* **81**, 3811 (1998).
- [6] J. Klaers, J. Schmitt, F. Vewinger, and M. Weitz, Bose-Einstein condensation of photons in an optical microcavity, *Nature (London)* **468**, 545 (2010).
- [7] L. V. Butov, A. L. Ivanov, A. Imamoglu, P. B. Littlewood, A. A. Shashkin, V. T. Dolgoplov, K. L. Campman, and A. C. Gossard, Stimulated scattering of indirect excitons in coupled quantum wells: Signature of a degenerate Bose-gas of excitons, *Phys. Rev. Lett.* **86**, 5608 (2001).
- [8] J. Kasprzak, M. Richard, S. Kundermann, A. Baas, P. Jeambrun, J. M. J. Keeling, F. M. Marchetti, M. H. Szymańska, R. André, J. L. Staehli *et al.*, Bose-Einstein condensation of exciton polaritons, *Nature (London)* **443**, 409 (2006).
- [9] S. O. Demokritov, V. E. Demidov, O. Dzyapko, G. A. Melkov, A. A. Serga, B. Hillebrands, and A. N. Slavin, Bose-Einstein condensation of quasi-equilibrium magnons at room temperature under pumping, *Nature (London)* **443**, 430 (2006).
- [10] E. B. Sonin, Superfluid spin transport in magnetically ordered solids (Review article), *Low Temp. Phys.* **46**, 436 (2020).
- [11] J. T. Mäkinen, S. Autti, and V. B. Eltsov, Magnon Bose-Einstein condensates: From time crystals and quantum chromodynamics to vortex sensing and cosmology, *Appl. Phys. Lett.* **124**, 100502 (2024).
- [12] S. Autti, V. V. Dmitriev, J. T. Mäkinen, J. Rysti, A. A. Soldatov, G. E. Volovik, A. N. Yudin, and V. B. Eltsov, Bose-Einstein condensation of magnons and spin superfluidity in the polar phase of ^3He , *Phys. Rev. Lett.* **121**, 025303 (2018).
- [13] A. A. Serga, V. S. Tiberkevich, C. W. Sandweg, V. I. Vasyuchka, D. A. Bozhko, A. V. Chumak, T. Neumann, B. Obry, G. A. Melkov, A. N. Slavin, and B. Hillebrands, Bose-Einstein condensation in an ultra-hot gas of pumped magnons, *Nat. Commun.* **5**, 3452 (2014).
- [14] D. A. Bozhko, A. J. E. Kreil, H. Yu. Musiienko-Shmarova, A. A. Serga, A. Pomyalov, V. S. L'vov, and B. Hillebrands, Bogoliubov waves and distant transport of magnon condensate at room temperature, *Nat. Commun.* **10**, 2460 (2019).
- [15] M. Schneider, T. Brächer, D. Breitbach, V. Lauer, P. Pirro, D. A. Bozhko, H. Yu. Musiienko-Shmarova, B. Heinz, Q. Wang, T. Meyer *et al.*, Bose-Einstein condensation of quasiparticles by rapid cooling, *Nat. Nanotechnol.* **15**, 457 (2020).
- [16] M. Schneider, D. Breitbach, R. O. Serha, Q. Wang, A. A. Serga, A. N. Slavin, V. S. Tiberkevich, B. Heinz, B. Lägél, T. Brächer, C. Dubs, S. Knauer, O. V. Dobrovolskiy, P. Pirro, B. Hillebrands, and A. V. Chumak, Control of the Bose-Einstein condensation of magnons by the spin Hall effect, *Phys. Rev. Lett.* **127**, 237203 (2021).
- [17] B. Divinskiy, H. Merbouche, V. E. Demidov, K. O. Nikolaev, L. Soumah, D. Gouéré, R. Lebrun, V. Cros, J. B. Youssef, P. Bortolotti *et al.*, Evidence for spin current driven Bose-Einstein condensation of magnons, *Nat. Commun.* **12**, 6541 (2021).
- [18] Y. Tabuchi, S. Ishino, A. Noguchi, T. Ishikawa, R. Yamazaki, K. Usami, and Y. Nakamura, Quantum magnonics: The

- magnon meets the superconducting qubit, *C. R. Phys.* **17**, 729 (2016).
- [19] Ö. O. Soykal and M. E. Flatté, Strong field interactions between a nanomagnet and a photonic cavity, *Phys. Rev. Lett.* **104**, 077202 (2010).
- [20] X. Zhang, C.-L. Zou, L. Jiang, and H. X. Tang, Strongly coupled magnons and cavity microwave photons, *Phys. Rev. Lett.* **113**, 156401 (2014).
- [21] Y. Yang, Yi-Pu Wang, J. W. Rao, Y. S. Gui, B. M. Yao, W. Lu, and C.-M. Hu, Unconventional singularity in anti-parity-time symmetric cavity magnonics, *Phys. Rev. Lett.* **125**, 147202 (2020).
- [22] S. Sharma, Y. M. Blanter, and G. E. W. Bauer, Optical cooling of magnons, *Phys. Rev. Lett.* **121**, 087205 (2018).
- [23] T. Liu, X. Zhang, H. X. Tang, and M. E. Flatté, Optomagnonics in magnetic solids, *Phys. Rev. B* **94**, 060405(R) (2016).
- [24] F. Šimić, S. Sharma, Y. M. Blanter, and G. E. W. Bauer, Coherent pumping of high-momentum magnons by light, *Phys. Rev. B* **101**, 100401(R) (2020).
- [25] N. Zhu, X. Zhang, X. Han, C.-L. Zou, and H. X. Tang, Inverse Faraday effect in an optomagnonic waveguide, *Phys. Rev. Appl.* **18**, 024046 (2022).
- [26] V. E. Zakharov, V. S. L'vov, and G. E. Falkovich, *Kolmogorov Spectra of Turbulence I* (Springer-Verlag, Berlin, 1992).
- [27] A. J. E. Kreil, D. A. Bozhko, H. Yu. Musienko-Shmarova, V. I. Vasyuchka, V. S. L'vov, A. Pomyalov, B. Hillebrands, and A. A. Serga, From kinetic instability to Bose-Einstein condensation and magnon supercurrents, *Phys. Rev. Lett.* **121**, 077203 (2018).
- [28] G. A. Melkov, V. L. Safonov, A. Yu. Taranenko, and S. V. Sholom, Kinetic instability and Bose condensation of nonequilibrium magnons, *J. Magn. Magn. Mater.* **132**, 180 (1994).
- [29] S. M. Rezende, Theory of coherence in Bose-Einstein condensation phenomena in a microwave-driven interacting magnon gas, *Phys. Rev. B* **79**, 174411 (2009).
- [30] A. Osada, R. Hisatomi, A. Noguchi, Y. Tabuchi, R. Yamazaki, K. Usami, M. Sadgrove, R. Yalla, M. Nomura, and Y. Nakamura, Cavity optomagnonics with spin-orbit coupled photons, *Phys. Rev. Lett.* **116**, 223601 (2016).
- [31] K. B. Davis, M. O. Mewes, M. R. Andrews, N. J. van Druten, D. S. Durfee, D. M. Kurn, and W. Ketterle, Bose-Einstein condensation in a gas of sodium atoms, *Phys. Rev. Lett.* **75**, 3969 (1995).
- [32] C. C. Bradley, C. A. Sackett, J. J. Tollett, and R. G. Hulet, Evidence of Bose-Einstein condensation in an atomic gas with attractive interactions, *Phys. Rev. Lett.* **75**, 1687 (1995).
- [33] F. Dalfovo, S. Giorgini, L. P. Pitaevskii, and S. Stringari, Theory of Bose-Einstein condensation in trapped gases, *Rev. Mod. Phys.* **71**, 463 (1999).
- [34] Yu. Kagan, G. V. Shlyapnikov, and J. T. M. Walraven, Bose-Einstein condensation in trapped atomic gases, *Phys. Rev. Lett.* **76**, 2670 (1996).
- [35] E. P. Gross, Structure of a quantized vortex in boson systems, *Il Nuovo Cimento (1955-1965)* **20**, 454 (1961).
- [36] L. P. Pitaevskii, Vortex lines in an imperfect Bose gas, *J. Exptl. Theoret. Phys. (U.S.S.R.)* **40**, 646 (1961) [*Sov. Phys. JETP* **13**, 451 (1961)].
- [37] V. S. L'vov, *Wave Turbulence Under Parametric Excitation: Applications to Magnets*, Springer Series in Nonlinear Dynamics (Springer, Berlin, Heidelberg, 1994).
- [38] O. Dzyapko, I. Lisenkov, P. Nowik-Boltyk, V. E. Demidov, S. O. Demokritov, B. Koene, A. Kirilyuk, T. Rasing, V. Tiberkevich, and A. Slavin, Magnon-magnon interactions in a room-temperature magnonic Bose-Einstein condensate, *Phys. Rev. B* **96**, 064438 (2017).
- [39] S. M. Rezende and F. M. de Aguiar, Spin-wave instabilities, auto-oscillations, and chaos in yttrium-iron-garnet, *Proc. IEEE* **78**, 893 (1990).
- [40] S. M. Rezende, *Fundamentals of Magnonics*, Lecture Notes in Physics (Springer International Publishing, Cham, 2020), Vol. 969.
- [41] V. E. Demidov, O. Dzyapko, S. O. Demokritov, G. A. Melkov, and A. N. Slavin, Thermalization of a parametrically driven magnon gas leading to Bose-Einstein condensation, *Phys. Rev. Lett.* **99**, 037205 (2007).
- [42] B. E. Storey, A. O. Tooke, A. P. Cracknell, and J. A. Przystawa, The determination of the frequencies of magnetostatic modes in rectangular thin films of ferrimagnetic yttrium iron garnet, *J. Phys. C* **10**, 875 (1977).
- [43] K. Yu. Guslienko, S. O. Demokritov, B. Hillebrands, and A. N. Slavin, Effective dipolar boundary conditions for dynamic magnetization in thin magnetic stripes, *Phys. Rev. B* **66**, 132402 (2002).
- [44] X. Zhang, C. Zou, L. Jiang, and H. X. Tang, Superstrong coupling of thin film magnetostatic waves with microwave cavity, *J. Appl. Phys.* **119**, 023905 (2016).
- [45] C. B. de Araujo, Quantum-statistical theory of the nonlinear excitation of magnons in parallel pumping experiments, *Phys. Rev. B* **10**, 3961 (1974).
- [46] P. Meystre and M. Sargent, *Elements of Quantum Optics*, 4th ed. (Springer, Berlin, Heidelberg, 2007).